Pacific Science (1982), vol. 36, no. 3

The Biomechanics of the Arteries of *Nautilus*, *Nototodarus*, and *Sepia*[1]

JOHN M. GOSLINE[2] and ROBERT E. SHADWICK[2]

ABSTRACT: The mechanical properties of the dorsal aorta of three cephalopod mollusks, *Nautilus pompilius*, *Nototodarus sloani*, and *Sepia latimanus*, were investigated by in vitro inflations of isolated arterial segments. As expected, all three arteries exhibit nonlinear, J-shaped stress–extension curves, and all are highly extensible in the circumferential direction. Differences in longitudinal extensibility appear to be correlated to specific features of the tissue architecture. The squid, *Nototodarus*, and to a lesser extent the cuttlefish, *Sepia*, arteries are reinforced longitudinally with a dense layer of longitudinally oriented elastic fibers.

Analysis of the form of the incremental wall stiffness data for *Nautilus* and *Nototodarus* suggests that the in vivo blood pressures for these animals fall in the ranges 20–60 cm H_2O and 100–200 cm H_2O, respectively. *Nautilus* has a thin-walled, low-pressure arterial system that is in keeping with its relatively limited locomotory capabilities. *Nototodarus* has a high-pressure, thick-walled circulation that is required to support the high-speed, aerobic locomotion generally common in squid. Analysis of pressure wave velocities for these arteries indicates that the *Nautilus* circulatory system contains a true *Windkessel* whereas it appears possible that wave propogation effects may make a relatively minor contribution to the hemodynamics of *Nototodarus*.

THE ROLE OF ELASTIC ARTERIES in the circulation of vertebrates has been known for many years. At its simplest, the rubberlike elasticity of the arteries provides a mechanism in which some of the energy released in the pulsatile contractions of the heart is stored. This stored energy can then be used in maintaining the flow of blood to the tissues during the refilling phase of the cardiac cycle (McDonald 1974). In order for a system of elastic arteries to function efficiently, the arteries must be relatively easy to inflate, so the heart will not have to work against a large systemic pressure. Therefore, the modulus of elasticity of the material from which the artery is constructed must be quite low. However, the cylindrical geometry of the artery imposes some very important constraints on the mechanical properties of the artery wall material. If the vessel is to inflate in a uniform, stable manner along its entire length and not "balloon out" in forming aneurisms, then the stiffness of the artery wall must increase sharply with radial expansion over the physiological range of extensions (Gosline 1980, Wainwright et al. 1976). Thus, arteries always show nonlinear, J-shaped stress–extension curves, and in higher vertebrates the incremental stiffness or incremental modulus of elasticity (E_{inc}) will increase with roughly the fifth power of radius in the physiological range (Bergel 1961). This dramatic shift in elastic properties is achieved by the parallel arrangement of a low-modulus, rubbery material (elastin) with a very stiff fiber (collagen) (Roach and Burton 1957). At low extensions (i.e., at low pressures) the collagen fibers are somewhat coiled and do not act to resist the internal pressure. The elastic properties of the composite are

[1] This research was conducted as part of the *Alpha Helix* Cephalopod Expedition to the Republic of the Philippines, supported by National Science Foundation grant PCM 77-16269 to J. Arnold. This study was also supported in part by Natural Sciences and Engineering Research Council of Canada grant 67-6934 to J. M. Gosline.

[2] University of British Columbia, Department of Zoology, Vancouver, British Columbia, Canada V6T 2A9.

dominated by the elastin and the modulus is low [of the order of 10^5 N m^{-2} (Newtons per square meter)]. As pressure increases and the artery is inflated, the collagen fibers become straightened and begin to resist the internal pressure. At the upper end of the physiological range of pressures the stiffness has increased by roughly an order of magnitude to about 10^6 N m^{-2}, and this dramatic increase in stiffness occurs over a range of radial expansion of the order of 25%. Clearly, the precise design of the arterial wall material is an essential component in the vertebrate circulatory system.

Until very recently, virtually nothing was known about the mechanics of the circulation in any invertebrate. Cephalopod mollusks have fairly complex, high-pressure, closed circulatory systems, and it is likely that elastic arteries may function in the cephalopods in much the same manner as they do in the vertebrates. The available blood pressure data (Bourne, Redmond, and Johansen 1978; Johansen and Martin 1962) suggest that elastic arteries are present in the octopus and in *Nautilus*. Shadwick (1978, 1980) and Shadwick and Gosline (1981) have recently shown that the dorsal aorta of *Octopus dofleini* is indeed elastic and that the animal makes use of the system's elasticity in maintaining blood flow during the entire cardiac cycle. Octopus arterial tissue exhibits a J-shaped stress–extension curve that is matched to the normal range of blood pressures in the animal. In addition, the arterial wall material is constructed from a protein rubber (not elastin, but a previously undescribed material) arranged in parallel with collagen fibers. Thus, it seems that the basic biophysical requirements of a closed, pulsatile circulatory system have led the cephalopods to evolve an arterial tree that is functionally analogous to the vertebrate system. This conclusion, however, is based on observations of a very sedentary animal, the octopus, and this animal may not correctly represent the more active cephalopods. This paper, therefore, presents a mechanical analysis of the major arteries of a squid (*Nototodarus sloani*), a cuttlefish (*Sepia latimanus*), and *Nautilus pompilius*.

MATERIALS AND METHODS

Experimental animals were purchased alive and in good condition from fishermen on the east coast of the island of Negros in the southern Philippines. Arterial tissues sampled for histology were dissected from the dorsal aorta just anterior to the systemic heart and were placed directly in Bouin's fixative. The tissues were dehydrated, embedded in wax, and sectioned according to standard histological techniques. The sections were stained using the Gomori aldehyde-fuchsin method (Cameron and Steele 1959). This staining procedure has been shown to preferentially stain the elastic fibers in the octopus aorta, leaving the muscle cells and the collagen fibers essentially unstained.

Arterial tissue isolated for mechanical tests was quickly dissected from freshly killed animals and placed in seawater at ambient temperatures (appox. 30°C). *Nautilus* artery samples were normally 4–6 cm long, and squid samples were usually 2–3 cm long. In all cases, as much of the dorsal aorta as could be easily isolated was used.

In inflation tests, the proximal end (toward the heart) of the sample was fitted over a piece of polyethylene tubing of the appropriate size and tied in place with surgical silk. The distal end and any small branch arteries were tied off with fine surgical silk. The polyethylene tubing was attached to either a seawater-filled or mercury-filled manometer, and the luminal pressure of the isolated arterial segment was measured as the height of the fluid reservoir above the specimen. The specimen was placed untethered under seawater in a wax-filled petri dish on the stage of a Wild M-3 stereomicroscope, and a Wild filar micrometer eyepiece (15×) was used to measure the longitudinal and radial expansion of the artery under pressure. Radial expansion was followed by observing the change in the outside diameter at a single recognizable point along the artery. Longitudinal expansion was followed by observing the change in separation of two small (approx. 5-μm wide) metal slivers that were inserted through the very outer layers of the artery wall. These markers were placed about

1 mm on either side of the point at which the radial expansion measurements were taken. The micrometer eyepiece gave excellent precision and reproducibility, and we estimate that the expansion measurements are accurate to better than about 2%. Wall thickness was determined by cutting a small ring sample of the artery from the area where the radial and longitudinal expansion measurements had been taken. The ring sample was turned on its side, and 15–20 measurements of wall thickness were taken at various points around the ring. The average value was taken to be the true wall thickness of the uninflated artery. The wall thickness of the inflated artery was calculated from the radial and longitudinal expansion values by assuming that the volume of the arterial wall material remained constant.

Before measurements were taken on an artery, the specimen was preloaded through several cycles to pressures that were greater than or equal to the highest pressures for which measurements were taken. This procedure has been shown to be necessary to obtain consistent, repeatable results with vertebrate arteries. Measurements were then taken, with pressure being increased and then decreased in a series of small increments. The specimen was held at each pressure for about 2 min to ensure that equilibrium values of expansion were obtained. In some cases, the artery showed clear signs of muscular activity, as indicated by a decrease in radius with increasing pressure. When this occurred, a few drops of ethanol were added to the seawater in the petri dish to anesthetize the specimen. In all cases, a few minutes after this treatment there was no evidence of muscular activity.

Force–extension tests were run on a small, portable tensile testing machine that extended the sample at a constant rate (typically about 1 mm/min). The force required to achieve the extension was detected by a strain gauge force transducer and recorded on a potentiometric pen recorder. Arterial samples tested in the longitudinal direction were attached to the test apparatus both by gluing with cyanoacrylate cement and by mechanical clamping. *Nautilus* arteries are large enough that it was possible to carry out tensile tests in the circumferential direction. This was done by cutting ring samples of the artery (approx. 1 cm long) and mounting the rings over stiff metal loops that were attached to the tensile test apparatus. In the case of both longitudinal and circumferential force–extension tests, the rate of extension was kept as low as possible (usually less than 10%/min) so that the measurements would at least approximate equilibrium values.

In both inflation and force–extension measurements, the extension of the sample is expressed in terms of longitudinal and circumferential extension ratios, $\lambda_L = L/L_0$ and $\lambda_C = R/R_0$, respectively (where L is length, R is radius, and L_0 and R_0 are the initial values of length and radius). Wall stress for the inflation tests was determined as follows (Wainwright et al. 1976):

$$\sigma_C = PR_i/T \quad (1)$$

$$\sigma_L = \sigma_C/2 \quad (2)$$

where σ_C is the circumferential stress, P is the pressure, R_i is the internal radius, T is the wall thickness, and σ_L is the longitudinal wall stress. Stress in the force–extension tests was defined as

$$\sigma = F/A \quad (3)$$

where F is the force and A is the instantaneous cross-sectional area of the specimen normal to the applied force. It was assumed that the material deforms without any significant change in volume, so A was calculated as

$$A = A_0/\lambda_L \quad (4)$$

where A_0 is the cross-sectional area of the undeformed sample.

RESULTS AND DISCUSSION

Figure 1 shows some typical pressure versus radial expansion data for *Nautilus* and for *Nototodarus* dorsal aorta. Although the form of this plot does not allow us to make any direct inferences about the properties of the arterial wall materials in these two animals, the general shape of the curves suggests that

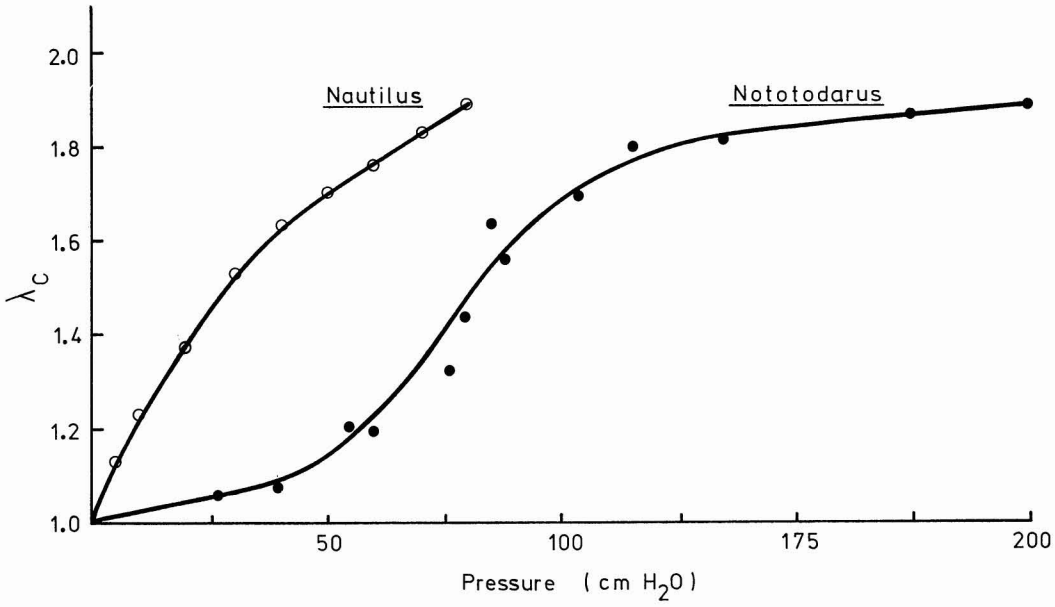

FIGURE 1. Circumferential expansion (λ_C) plotted against luminal pressure for untethered segments of dorsal aorta from *Nautilus* and from the squid *Nototodarus*.

the *Nautilus* artery, and hence the *Nautilus* circulatory system, is designed to function at low pressures while the squid artery and circulatory system probably function at higher pressures. However, beyond this very qualitative assessment, these data do not allow us to make any detailed predictions about the blood pressure or other hemodynamic parameters in these animals.

To assess the mechanical properties of the arterial wall material it is necessary to convert the pressure–radius data into wall stress and extension ratios. A typical plot of circumferential wall stress against circumferential extension ratio for *Nautilus* dorsal aorta is plotted in Figure 2. The nonlinear, J-shaped stress–extension curve that is characteristic of all arteries is readily apparent. Data are presented for both the inflation (increasing stress) and deflation phases of the cycle, as indicated by the arrows. This graph allows us to assess one very important aspect of the arterial elastic properties, namely the resilience or the efficiency of elastic energy storage in the arterial wall. The area under the stress–extension curve for the inflation phase (A_i)

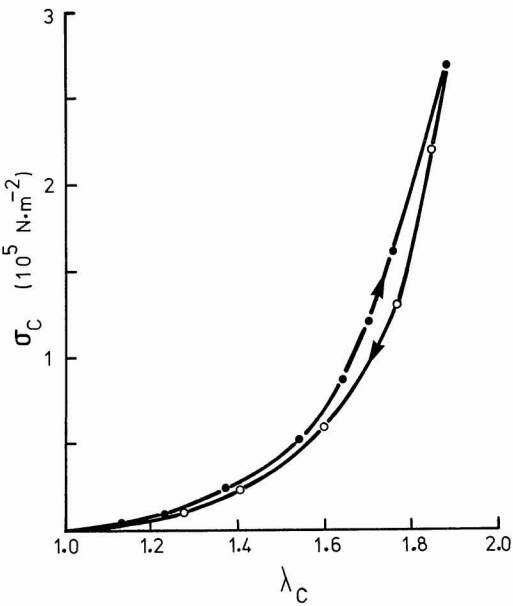

FIGURE 2. Circumferential wall stress (σ_C) versus circumferential extension ratio (λ_C) for *Nautilus* dorsal aorta. Data were collected for an untethered sample for both inflation (closed symbols) and deflation (open symbols). Resilience of the inflation–deflation cycle is about 86%.

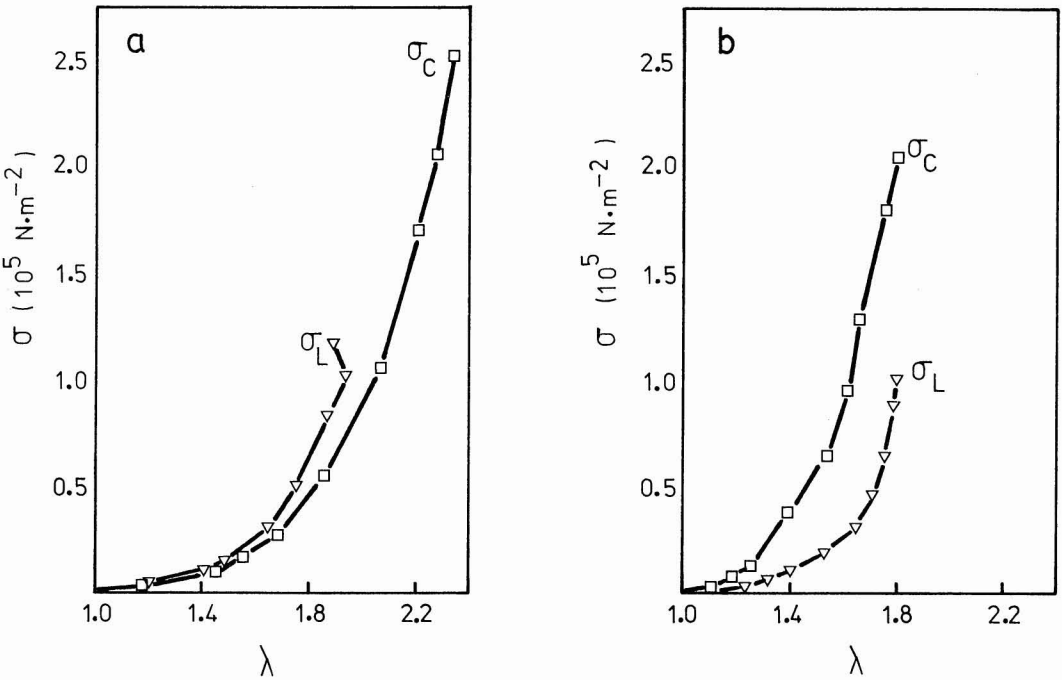

FIGURE 3. Biaxial stress–extension data for *Nautilus* aorta. *a*, properties of the aorta about 1 cm anterior to the heart; *b*, properties of the same aorta about 4.5 cm anterior to the heart; σ_L is the longitudinal stress, σ_C is the circumferential stress, and λ is the extension ratio. In each case, circumferential stress values are plotted against circumferential extension ratio, and longitudinal stress values are plotted against longitudinal extension ratio.

gives the elastic energy stored, and the area under the deflation curve (A_d) gives the energy recovered. Thus, the ratio A_d/A_i gives a measure of the efficiency of elastic energy storage, and this ratio turns out to be about 0.86, or 86% resilience, for the *Nautilus* artery. This is a high resilience that compares well with values for many high-quality, synthetic rubbers. However, note that this value of resilience was obtained under essentially static conditions, and when loaded dynamically (i.e., at the pulse frequency of the animal) the resilience of the material may be somewhat lower. Still, these values are similar to values found for vertebrate arteries, and thus it seems reasonable to conclude that this artery is capable of storing elastic energy in the normal functioning of the animal's circulatory system. Although we will not present any further information on arterial resilience, our measurements with squid and cuttlefish arteries indicate that these animals also have efficient elastic structures in their circulatory systems. In the stress–extension plots that follow we will present data only for the inflation phase of the cycle so that we can concentrate on the relationship between tissue architecture and arterial mechanical properties.

One interesting and probably very important aspect of the design of cephalopod arteries is that they can expand in length as well as in diameter when they are inflated. This situation is in sharp contrast to the case in virtually all vertebrate arteries, because vertebrate arteries in vivo are pretensioned in the longitudinal direction through rigid attachments to the skeletal system. This longitudinal pretensioning apparently prevents the arteries from getting longer during a pressure pulse from the heart, since in vivo observations indicate that there are no changes in length. However, if vertebrate arteries are inflated in vitro without longitudinal pretension, then the arteries do get longer. The situation is probably quite different in the cephalopods. Cephalopods

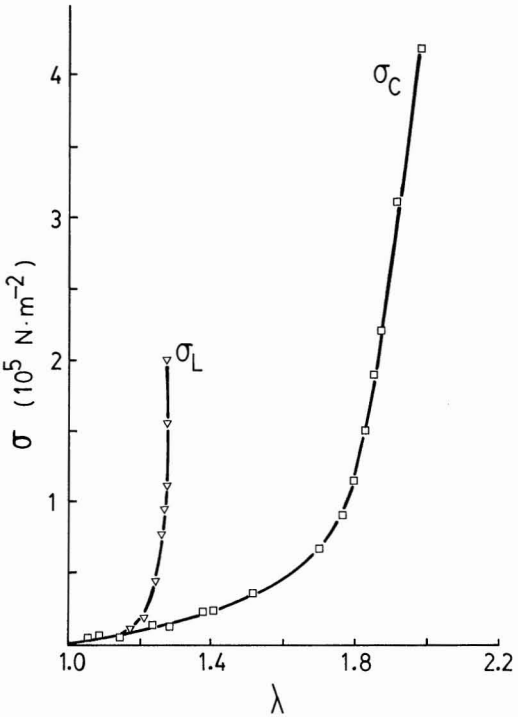

FIGURE 4. Biaxial stress–extension data for inflation of the dorsal aorta of *Sepia latimanus*; σ_L is the longitudinal stress, σ_C is the circumferential stress, and λ is the extension ratio. Circumferential stress is plotted against circumferential extension ratio, and longitudinal stress is plotted against longitudinal extension ratio.

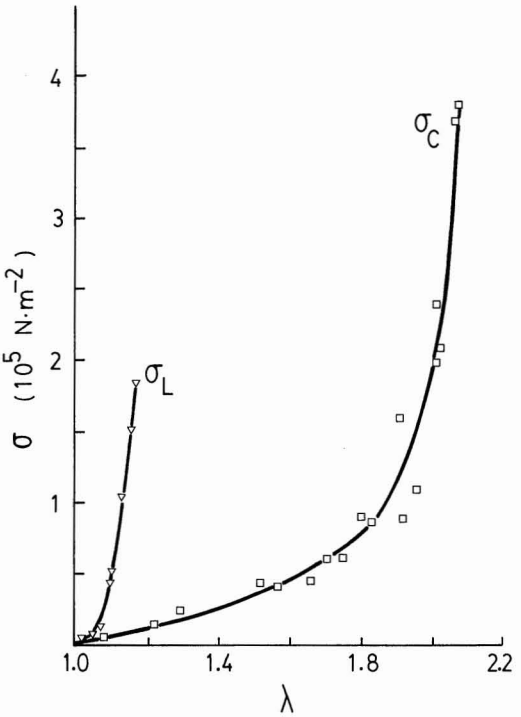

FIGURE 5. Biaxial stress–extension data for inflation of the dorsal aorta of *Nototodarus sloani*; σ_L is the longitudinal stress, σ_C is the circumferential stress, and λ is the extension ratio. Circumferential stress is plotted against circumferential extension ratio, and longitudinal stress is plotted against longitudinal extension ratio.

have few, if any, stiff skeletal elements to which their arteries may be tethered, so we suspect that in vitro inflations of untethered arteries will probably provide a good indication of the properties of the arteries in vivo.

Figures 3–5 show biaxial stress–extension data for individual dorsal aortas from *Nautilus*, *Sepia*, and *Nototodarus*, respectively. The *Nautilus* data show results from two positions along the same artery. The data in Figure 3*a* show the properties of the artery about 1 cm anterior to the heart, while the data in Figure 3*b* show the properties about 4.5 cm anterior to the heart, close to the site where the dorsal aorta enters the head region. The circumferential stress–extension (σ_C versus λ_C) curves indicate that the dorsal aortas of all three animals are very extensible in the radial direction, with radial expansions ranging from 80% to more than 120% for the pressures used. On the other hand, the longitudinal stress–extension (σ_L versus λ_L) curves indicate that there is considerable variation in longitudinal extensibility. We suspect that the differences in longitudinal extensibility reflect important design parameters of each animal's skeletal and circulatory systems. In general, arteries from octopus (Shadwick and Gosline 1981) and *Nautilus* show very large longitudinal expansions in untethered inflations, while arteries from *Sepia* and *Nototodarus* show very small length changes in untethered inflations. In fact, the cuttlefish and squid arteries seem to approach the state that pretensioned vertebrate arteries achieve. However, they do this not by tethering to a stiff skeleton, but by appropriate construction of the arterial wall material itself.

Extensible arteries in the octopus may be associated with the "floppy" skeletal system,

which is deformed in many different ways as the animal crawls into small crevices, etc. Clearly, an extensible aorta is essential if the circulatory system is to conform to these changes in body shape. In addition, longitudinal expansions brought about by pressure pulses from the heart can store elastic energy as well as radial expansions. The situation with *Nautilus* is probably somewhat different, since the animal lives encased in a rigid shell. However, the soft tissues inside the shell are deformable, and it is likely that the arterial tree is stretched during the normal movements of the animal inside its shell. In addition, the dorsal aorta follows a sinuous path anteriorly toward the head and appears to be only loosely attached to the various soft tissues between which it passes. In other words, *Nautilus*, like the octopus, is constructed in such a way that the aorta expands in length.

The situation is very different in the squid and the cuttlefish. The dorsal aorta passes anteriorly through the digestive gland in a direct path toward the head, and it appears to be attached firmly to the tissues through which it passes. In addition, it seems likely that the mantle/pen and mantle/cuttlebone structures of the squid and cuttlefish, respectively, prevent normal body movements from causing any substantial changes in the length of the aorta. Indeed, the analysis that follows suggests that the aorta of *Nototodarus* functions at the very steepest part of the σ_L versus λ_L curve in Figure 5 and that the artery lengthens by less than about 2% during a normal pressure pulse in vivo. The situation is probably the same in *Sepia*, but the *Nautilus* aorta may lengthen by as much as 35%. Although the exact role of these differences in mechanical properties is beyond the scope of this study, it seems clear that these differences are both real and significant. It remains to consider how these differences arise.

The structural basis for the mechanical properties of the arteries is illustrated by the graphs of the stress–extension data in Figures 3–5. Normally, the slope of a stress–extension curve gives the stiffness or modulus of elasticity ($E = \Delta\sigma/\Delta\lambda$) of the material being tested, and then the stiffness values can be correlated directly with the observed tissue architecture, etc. In the case of inflations of cylindrical tubes, the situation becomes considerably more complex, because an internal pressure applies loads in two directions simultaneously (i.e., longitudinally and circumferentially). The longitudinal extension (λ_L) and the circumferential extension (λ_C) that result from this biaxial loading depend on the longitudinal stiffness (E_L), the circumferential stiffness (E_C), and the interaction between the longitudinal and circumferential extensions. This last variable is expressed as Poisson's ratio (ν), which is the ratio of the lateral contraction divided by the longitudinal extension in a uniaxial extension test. For example, when a rubber band is stretched uniaxially it gets longer and thinner, and for small extensions $\nu = 0.50$. In the biaxial expansion of a cylinder the lateral contraction associated with the circumferential expansion (i.e., the contraction in the longitudinal direction) will tend to counteract the action of the pressure to make the cylinder longer, and vice versa. This makes the interpretation of the stress–extension data in Figures 3–5 difficult. The σ_L versus λ_L curve in Figure 4 for σ_L values of 10^5 N m^{-2} and greater is vertical, suggesting an infinite modulus. Similarly, the slope of the line connecting the last two σ_L points in Figure 3*a* suggests a negative modulus (i.e., the artery got shorter when the pressure was increased). These apparently anomalous observations arise from the biaxial interactions described above. When a simple, isotropic rubber tube (for which $E_L = E_C$, $\nu = 0.50$) is inflated, it will expand only in circumference because the lateral contraction associated with the circumferential expansion just balances the longitudinal extension. When a complex structure such as an artery is inflated, the exact solution to the problem becomes essentially unattainable. Dobrin and Doyle (1970) provide a method for estimating E_C, E_L, and ν from inflation data. The method is based on a number of assumptions, and the results should be taken only as approximations of the true values. Their method uses the following two equations:

$$\Delta\lambda_L = (\Delta\sigma_L/E_L) - \nu(\Delta\sigma_C/E_L) \quad (5)$$

$$\Delta\lambda_C = (\Delta\sigma_C/E_C) - \nu(\Delta\sigma_L/E_L) \quad (6)$$

where the $\Delta\lambda$ and $\Delta\sigma$ terms represent the longitudinal and circumferential changes in ex-

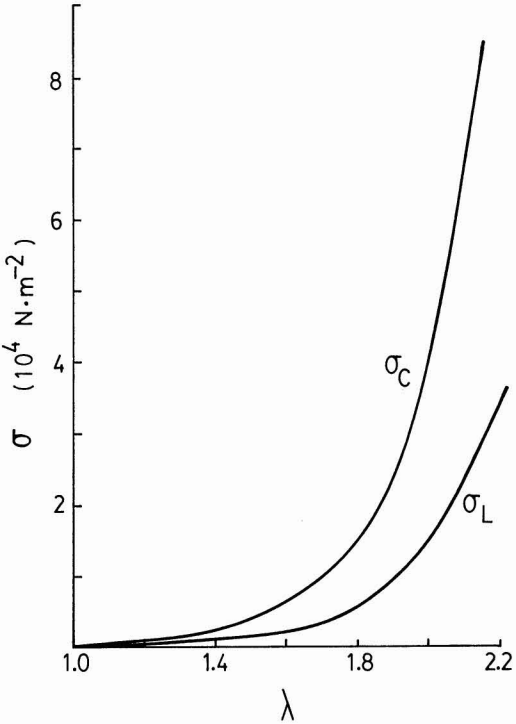

FIGURE 6. Uniaxial stress–extension data for *Nautilus* dorsal aorta extended circumferentially and longitudinally; σ_L is the longitudinal stress, σ_C is the circumferential stress, and λ is the extension ratio. Circumferential stress is plotted against circumferential extension ratio, and longitudinal stress is plotted against longitudinal extension ratio.

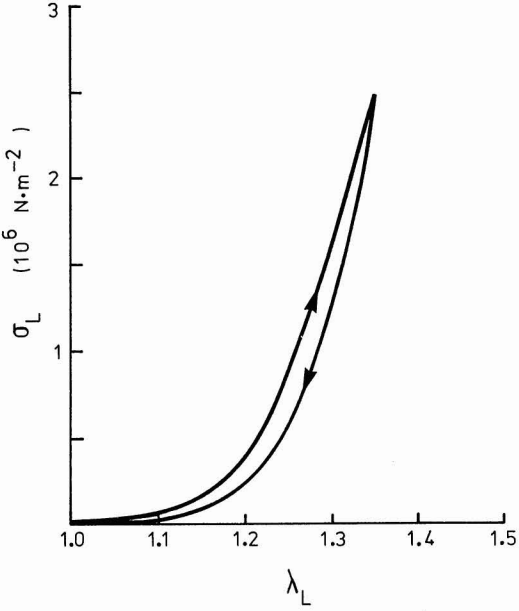

FIGURE 7. Uniaxial stress–extension data for *Nototodarus* dorsal aorta extended longitudinally; σ_L is the longitudinal stress and λ_L is the longitudinal extension ratio. Arrows indicate the loading and unloading phases of the cycle. Resilience for the cycle is about 76%.

tension and in stress for one increment of pressure in the pressure–inflation data. It is not possible to solve these two equations for all three unknowns (E_C, E_L, and ν), so estimates of E_L must be obtained from uniaxial stress–extension tests. It is then possible to solve for ν and E_C.

Figures 6 and 7 show uniaxial stress–extension curves for *Nautilus* and *Nototodarus* dorsal aortas, respectively. Values for the longitudinal modulus ($E_L = \Delta\sigma/\Delta\lambda$) derived from these curves were used to calculate ν and E_C, as outlined above, and the results of some typical calculations are shown in Tables 1 and 2. Table 1*a* shows calculations from the *Nautilus* data plotted in Figure 3*a*, and Table 1*b* shows calculations from the data in Figure 3*b*. Table 2 shows the calculations for the *Nototodarus* data plotted in Figure 5. Note first the ratio of the circumferential to longitudinal stiffness (E_C/E_L). For both sets of *Nautilus* data, this ratio is large (approx. 3.2–4.0) and nearly constant over the entire range of inflation pressures. This high stiffness ratio is consistent with the longitudinal and circumferential stress–extension data plotted in Figure 6, and probably explains why *Nautilus* arteries expand so much in length when they are inflated. Differences in the two sets of *Nautilus* data are small but are probably significant. Poisson's ratio and the modulus ratio are both smaller in Table 1*a* (the properties of the aorta closest to the heart) than in Table 1*b*, and these small differences account for the lower longitudinal extensibility of the proximal portion of the aorta. The situation in the squid is more complex. At low pressures the modulus ratio is about 0.5, indicating that the arterial wall material is stiffer in the longitudinal direction than in the circumferential direction. This probably explains why the *Nototodarus* aorta lengthens so little. As the pressure is increased to the middle of the

TABLE 1*a*

SUMMARY OF CALCULATED DATA FOR INFLATIONS OF *Nautilus* DORSAL AORTA; DATA COLLECTED ABOUT 1 cm ANTERIOR TO THE HEART (PROXIMAL)

λ_C	PRESSURE (cm H_2O)	E_L (N m^{-2})	ν	E_C (N m^{-2})	E_C/E_L	C (cm/sec)
1.18	5	1.0×10^3	0.46	3.3×10^3	3.28	68
1.45	10	1.8×10^3	0.46	5.8×10^3	3.22	67
1.56	15	3.5×10^3	0.42	1.4×10^4	3.95	88
1.69	20	5.0×10^3	0.47	1.7×10^4	3.36	89
1.86	30	1.0×10^4	0.44	3.6×10^4	3.63	109
2.05	40	2.3×10^4	0.45	7.4×10^4	3.30	133
2.20	50	3.5×10^4	0.44	1.1×10^5	3.21	147
2.28	60	6.0×10^4	0.38	1.9×10^5	3.20	190
2.34	70	—	—	—	—	—

TABLE 1*b*

SUMMARY OF CALCULATED DATA FOR INFLATIONS OF *Nautilus* DORSAL AORTA; DATA COLLECTED ABOUT 4.5 cm ANTERIOR TO THE HEART (DISTAL)

λ_C	PRESSURE (cm H_2O)	E_L (N m^{-2})	ν	E_C (N m^{-2})	E_C/E_L	C (cm/sec)
1.11	5	1.0×10^3	0.45	3.8×10^3	3.80	65
1.19	10	1.5×10^3	0.46	6.9×10^3	3.83	77
1.25	15	3.0×10^3	0.46	1.1×10^4	3.77	91
1.27	20	3.2×10^3	0.47	1.3×10^4	4.00	92
1.39	30	4.0×10^3	0.47	1.6×10^4	3.92	89
1.54	40	7.0×10^3	0.47	2.7×10^4	3.89	106
1.61	50	9.0×10^3	0.49	2.9×10^4	3.59	100
1.66	60	1.2×10^4	0.48	4.6×10^4	3.87	119
1.75	70	2.2×10^4	0.49	7.8×10^4	3.53	145
1.80	80	2.9×10^4	0.48	9.8×10^4	3.73	160

TABLE 2

SUMMARY OF CALCULATED DATA FOR INFLATIONS OF *Nototodarus* DORSAL AORTA

λ_C	PRESSURE (cm H_2O)	E_L (N m^{-2})	ν	E_C (N m^{-2})	E_C/E_L	C (cm/sec)
1.07	40	1.0×10^5	0.17	6.0×10^4	0.6	545
1.21	54	1.1×10^5	0.35	5.6×10^4	0.5	446
1.29	78	1.1×10^5	0.28	7.0×10^4	0.6	414
1.65	81	1.5×10^5	0.45	6.4×10^4	0.4	295
1.80	135	2.0×10^5	0.31	1.7×10^5	0.8	408
1.89	202	2.4×10^5	0.48	3.5×10^5	1.6	614
1.95	190	2.6×10^5	0.38	4.0×10^5	1.5	576
2.01	270	3.2×10^5	0.44	4.8×10^5	1.3	590
2.02	230	3.2×10^5	0.41	8.0×10^5	2.5	769
2.07	405	4.0×10^5	0.44	1.0×10^6	2.6	—
2.14	513	5.2×10^5	0.44	1.1×10^6	2.2	—

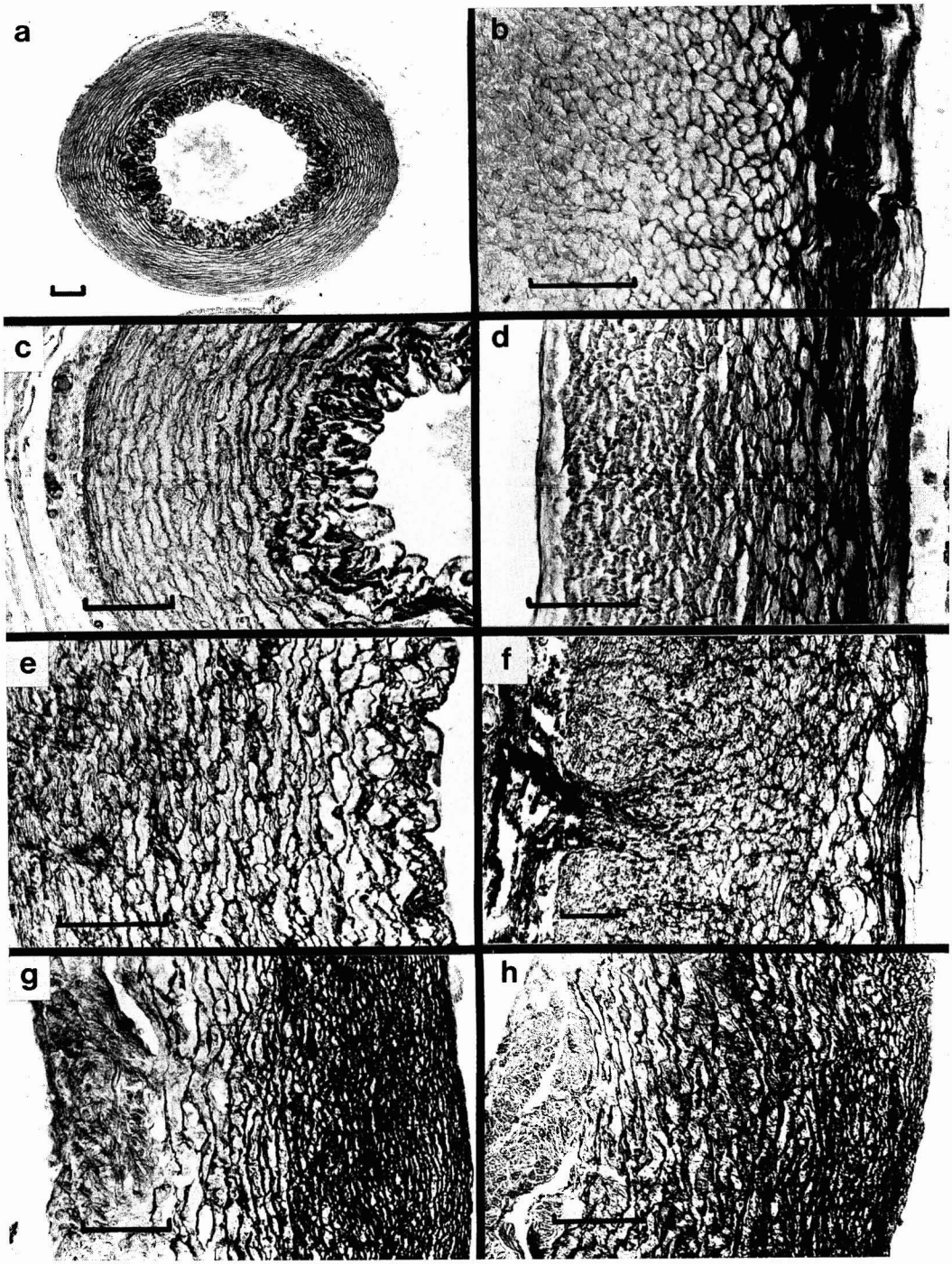

FIGURE 8. Light micrographs of the dorsal aortas of *Nototodarus* (*a* and *b*), *Sepioteuthis lessoniana* (*c* and *d*), *Sepia* (*e* and *f*), and *Nautilus* (*g* and *h*). All sections are stained with Gomori's aldehyde-fuchsin method to reveal the organization of the elastic fibers. Figures *a*, *c*, *e*, and *g* are cross sections with the luminal surface to the right, and figures *b*, *d*, *f*, and *h* are longitudinal sections with the luminal surface to the right. The scale bar is 100 μm in all figures.

range, the modulus ratio increases to about 1–1.5 and finally reaches values of 2–2.5 at the highest pressures.

These values of modulus ratio and Poisson's ratio are difficult to interpret on their own, but the micrographs in Figure 8 provide some helpful morphological information. (Note that these sections have been stained for the rubberlike elastic fibers and do not provide any information concerning the organization of collagen fibers or the muscle cells that fill the spaces between the elastic fibers.) The micrographs in Figure 8*a*, *c*, *e*, and *g* are cross sections with the luminal surface to the right. The micrographs in Figure 8*b*, *d*, *f*, and *h* are longitudinal sections with the luminal surface to the right. Cross sections of *Nautilus* arteries (Figure 8*g*) look very much like similar sections of typical vertebrate artery stained for elastin. There appear to be numerous lamellae of elastic material through the thickness of the artery wall, but most of the elastic tissue is concentrated in the inner two-thirds of the wall thickness. In longitudinal sections of *Nautilus* (Figure 8*h*) the wall looks much the same, suggesting that the elastic material in these lamellae are oriented equally in the longitudinal and circumferential directions. However, the modulus ratios given in Tables 1*a* and 1*b* indicate that this is not the case. Even at low pressures where the modulus of the tissue is very low (less than 10^4 N m^{-2}), the circumferential stiffness is three to four times greater than the longitudinal stiffness. Thus, we conclude that these lamellae are fibrillar at a level that is not resolved in these micrographs. Furthermore, the modulus ratio indicates either that circumferentially oriented fibers are about three to four times as abundant as longitudinal fibers, or more likely, that the fibers are arranged helically at an average fiber angle of about 72° to the long axis of the artery (i.e., $\tan^{-1} 3 = 72°$).

The appearance of the arteries from *Nototodarus* (Figure 8*a*, *b*), another squid (*Sepioteuthis lessoniana*; Figure 8*c*, *d*), and *Sepia* (Figure 8*e*, *f*) all look much like the *Nautilus* artery, particularly in the outer portion of the artery wall. The lamellar organization is clearly seen in cross sections, but is less apparent in longitudinal sections. This again suggests a preferred orientation of the elastic fibers in the lamellae that is closer to the circumferential direction. However, one difference in organization is apparent. There is a distinct inner layer of longitudinally oriented fibers. In *Nototodarus* and *Sepioteuthis lessoniana* the longitudinal fibers appear to be even denser and more abundant than the lamellae. They presumably account for the low modulus ratio seen at low pressures in Table 2 ($E_C/E_L = 0.5$ for *Nototodarus*), and they are undoubtedly responsible for limiting the longitudinal extensibility. The fact that the modulus ratio increases at moderate pressures and the tissue modulus approaches 10^6 N m^{-2} at the highest pressures suggests that collagen fibers arranged at large angles to the long axis of the artery begin to carry a substantial portion of the load at these pressures.

With this general understanding of the structural basis for the observed elastic properties, we may now turn our attention to determining the physiologically relevant region of the stress–extension curves. Vertebrate arteries function over a rather limited range of their stress–extension curves where the circumferential incremental modulus of elasticity (E_{inc}, as defined by Bergel 1961) increases very rapidly, and we believe that we can use this criterion to identify the functional range of cephalopod arteries as well. Accordingly, we have plotted circumferential E_{inc} ($E_{inc} = \lambda_C E_C$) against λ_C for arteries of *Nautilus* (Figure 9) and *Nototodarus* (Figure 10). The values are derived from the data in Tables 1 and 2. For the *Nautilus* proximal position the region of rapidly increasing E_{inc} seems to be in the range $\lambda_C = 1.6$ to $\lambda_C = 2.2$; for the more distal location the region of rapid increase appears to be in the range $\lambda_C = 1.4$ to $\lambda_C = 1.7$. These extensions correspond to pressures of 20–60 cm H_2O, and therefore we believe that this is the normal range of blood pressure for this animal. Pressure recordings available for *Nautilus* (Bourne et al. 1978) are in this range. In the case of the squid, the region of rapid increase in circumferential E_{inc} is in the range $\lambda_C = 1.70$ to $\lambda_C = 1.90$, and this corresponds to pressures of about 100–200 cm H_2O (or 74–148 mm Hg). It is surprising how close this pressure

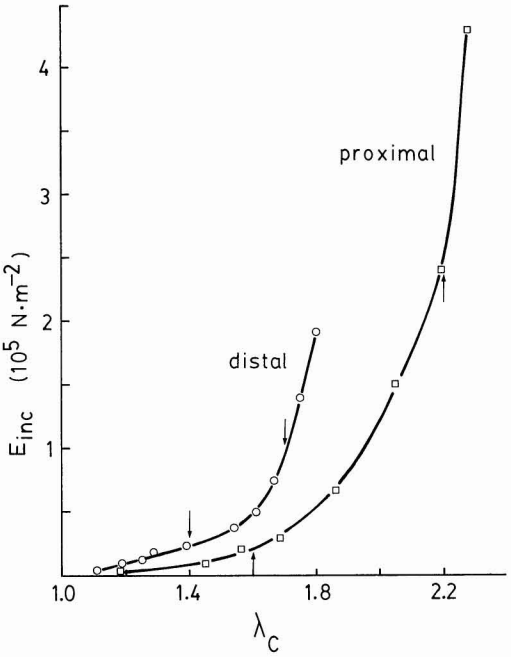

FIGURE 9. Circumferential incremental modulus (E_{inc}) as a function of circumferential extension ratio (λ_C) for *Nautilus* dorsal aorta. These values have been calculated from the inflation data shown in Figure 3, as outlined in the text. The curve labeled "proximal" corresponds to Figure 3*a*, and the curve labeled "distal" corresponds to Figure 3*b*. The arrows indicate the ranges of rapidly increasing E_{inc} used to estimate physiological pressures in this animal.

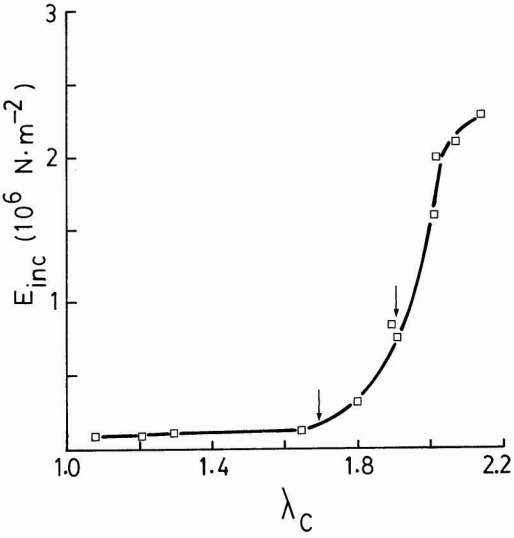

FIGURE 10. Circumferential incremental modulus (E_{inc}) as a function of circumferential extension ratio (λ_C) for *Nototodarus* dorsal aorta. The arrows indicate the range of rapidly increasing E_{inc} used to estimate physiological pressures in this animal.

range comes to the normal range for mammals, and indeed it is surprising how similar squid arteries are to mammalian arteries.

We can now compare the dimensions and properties of these arteries as they probably exist in vivo. Figure 11 shows diagrams of cross sections of *Nautilus*, *Nototodarus*, and *Sepia* arteries at zero pressure, low physiological pressure, and high physiological pressure. The diagram for *Sepia* was based largely on the squid data, since these animals are similar. The *Nautilus* and the squid from which these data were taken were almost identical in size (*Nautilus*: 490-g animal and 185-g shell; *Nototodarus*: 420-g animal), but the squid is certainly the more active of the two. In fact, the gross morphology of *Nototodarus* suggests that it is a very active squid. The arterial morphology (Figure 11) indicates two completely different circulatory strategies for these animals. *Nautilus* presents a large-volume, thin-walled arterial system that functions at very low pressures. These are characteristics of a more primitive, open circulatory system. The squid, on the other hand, looks very much like the system in active vertebrates, employing high pressures and thus requiring low-volume, thick-walled vessels. The cuttlefish aorta looks much like the squid aorta in wall thickness, but the size is larger because the animal from which this artery was obtained was much larger (1860 g) than the squid.

Finally, we can use the artery wall dimensions and circumferential elastic properties to determine whether cephalopod circulatory systems are of the *Windkessel* type (i.e., a single functional elastic reservoir) or of the wave-propagation type (see McDonald 1974 for a discussion of these terms). We must first determine the characteristic pressure wave velocity for the arteries, as

$$C = (0.67E_C T/\rho R_i)^{\frac{1}{2}} \qquad (7)$$

where C is the velocity, E_C is the circumferential elastic modulus, T is the wall thickness, ρ is the density of the blood (assumed to be

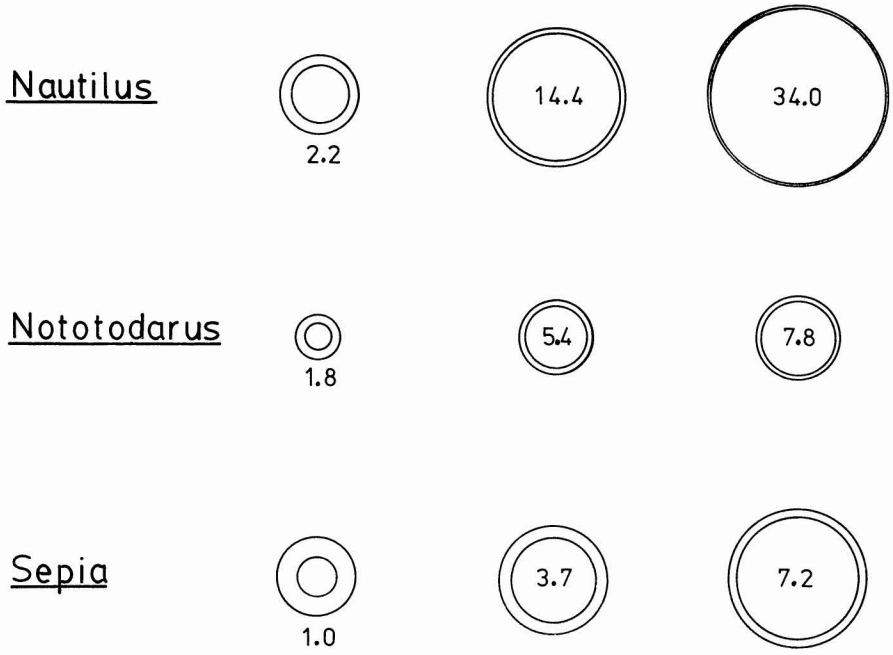

FIGURE 11. Diagrams representing cross sections of dorsal aortas from a 490-g *Nautilus*, a 420-g *Nototodarus*, and a 1860-g *Sepia* at zero pressure (to the left), low physiological pressure (middle), and high physiological pressure (to the right). The numbers indicate the ratio of the internal radius to the wall thickness (R_i/T).

about 1 g/cm^3), and R_i is the internal radius of the artery (Saito and Vander Werff 1975). Calculated values for the wave velocity are given in Tables 1 and 2. Average values in the physiological range are about 100 cm/sec for the *Nautilus* aorta and about 400 cm/sec for the *Nototodarus* aorta. The heart rate of *Nautilus* is of the order of 20 beats/min (i.e., 0.33 Hz; Bourne et al. 1978), and therefore the wavelength of the pressure wave in a *Nautilus* aorta will be of the order of 303 cm (i.e., 100 cm/sec ÷ 0.33/sec = 303 cm). Wave-propagation effects are important only when the length of the arterial tree is approximately one-quarter of the wavelength. Since the dorsal aorta of *Nautilus* is less than about 8 cm, wave propagation effects can contribute only to the tenth-order or higher harmonic components of the pressure wave. We conclude, therefore, that the *Nautilus* circulation functions as a single elastic reservoir, or *Windkessel*.

We do not know the true heart rate of a resting or actively swimming squid (Johansen and Martin 1962), but our estimates of squid blood pressure suggest that the squid circulatory system is similar to that of mammals. The heart rate for a mammal of equivalent size (e.g., a rat) suggests that a range of 60–180 beats/min (1–3 Hz; Spector 1965) might be appropriate for the squid. Taking these values as a first approximation, the shortest wavelength in the squid aorta would be about 130 cm. Since the total length of *Nototodarus* is typically about 25 cm, it is unreasonable to expect the dorsal aorta to be longer than about 8 cm (i.e., one-third of the total length). The quarter wavelength in *Nototodarus* will be about 32 cm, and therefore wave-propagation effects can contribute only to the fourth-order and higher harmonic components of the pressure wave. Although information is not available on the shape of the blood pressure wave in any squid, it is not unreasonable to expect that there are some small fourth-order harmonic components. Thus, wave-propagation effects may make some minor contributions to the hemodynamics of *Nototodarus*.

Other squids get much larger than *Nototodarus*, and if wall stiffness and the thickness/radius ratios remain the same, then other squids may well show more pronounced wave-propagation effects, as do all large, active vertebrates. This very interesting aspect of cephalopod circulatory dynamics certainly warrants further investigation.

LITERATURE CITED

BERGEL, D. H. 1961. The static elastic properties of the artery wall. J. Physiol. 156:445–457.

BOURNE, G. B., J. R. REDMOND, and K. JOHANSEN. 1978. Some aspects of hemodynamics in *Nautilus pompilius*. J. Exp. Zool. 205:63–70.

CAMERON, M. L., and J. E. STEELE. 1959. Simplified aldehyde-fuchsin staining of neurosecretory cells. Stain Technol. 34:265–266.

DOBRIN, P. B., and J. M. DOYLE. 1970. Vascular smooth muscle and anisotropy of dog carotid artery. Circ. Res. 27:105–119.

GOSLINE, J. M. 1980. The elastic properties of rubber-like proteins and highly extensible tissues. Pages 331–357 *in* J. F. V. Vincent and J. D. Currey, eds. The mechanical properties of biological materials. 34th Symp. Soc. Exp. Biol.

JOHANSEN, K., and A. W. MARTIN. 1962. Circulation in the cephalopod *Octopus dofleini*. Comp. Biochem. Physiol. 5:161–176.

MCDONALD, D. A. 1974. Blood flow in arteries. Edward Arnold, London.

ROACH, M. R., and A. C. BURTON. 1957. The reason for the shape of the distensibility curves of arteries. Can. J. Biochem. Physiol. 35:681–690.

SAITO, G. E., and T. J. VANDER WERFF. 1975. The importance of viscoelasticity in arterial blood flow models. J. Biomech. 8:237–245.

SHADWICK, R. E. 1978. A rubber-like protein from octopus arteries. Biorheol. 15:476.

———. 1980. Viscoelasticity and pulse wave velocity in the aorta of *Octopus dofleini*. Amer. Zool. 20:768.

SHADWICK, R. E., and J. M. GOSLINE. 1981. Elastic arteries in invertebrates: Mechanics of the octopus aorta. Science 213:759–761.

SPECTOR, W. S. 1965. Handbook of biology. W. B. Saunders, Philadelphia.

WAINWRIGHT, S. A., W. D. BIGGS, J. D. CURREY, and J. M. GOSLINE. 1976. Mechanical design in organisms. Edward Arnold, London.